Thermal Decomposition Kinetics of the Aviation Turbine Fuel Jet A

Jason A. Widegren and Thomas J. Bruno*

Physical and Chemical Properties Division, National Institute of Standards and Technology, 325 Broadway, Boulder, Colorado 80305-3328

As part of a large-scale thermophysical property measurement project, the global decomposition kinetics of the aviation turbine fuel Jet A was investigated. Decomposition reactions were performed at 375, 400, 425, and 450 °C in stainless steel ampule reactors. At each temperature, the extent of decomposition was determined as a function of time by gas chromatography. These data were used to derive global pseudo-first-order rate constants that approximate the overall decomposition rate of the mixture. Decomposition rate constants ranged from 5.9×10^{-6} s^{-1} at 375 °C to 4.4×10^{-4} s^{-1} at 450 °C. These rate constants are useful for planning property measurements at high temperatures. On the basis of the amount of time required for 1% of the sample to decompose ($t_{0.01}$), we found that allowable instrument residence times ranged from about 0.5 h at 375 °C to less than 1 min at 450 °C. The kinetic data were also used to derive Arrhenius parameters of $A = 4.1 \times 10^{12}$ s^{-1} and $E_a = 220$ kJ·mol^{-1}. In addition to the decomposition kinetics, we have also done a GC-MS analysis of the vapor phase that is produced during the thermal decomposition measurements.

Introduction

Kerosene-based aviation turbine fuels are the primary jet fuels for commercial airlines and military fleets.[1–5] The kerosene-based fuel supplied at commercial airports throughout the United States and parts of Canada is called Jet A (the specification for this fuel is ASTM D1655). A related fuel that is used commercially in most of the rest of the world is called Jet A-1. JP-8, which is essentially Jet A with an additive package,[4] is currently the primary jet fuel used by the United States military. However, there is a desire in the United States defense community to utilize JP-8 as the main battlefield fuel for all vehicles—not only for aviation applications but also for ground-based forces. For this reason, the physical and chemical properties of JP-8 are receiving renewed interest. By extension, the properties of Jet A are also receiving renewed interest because Jet A is the additive-free "base" fuel for JP-8.

Physical and chemical property data for aviation fuels are important for engineering design and process development.[6] The properties that are needed include equilibrium properties (such as fluid density, vapor pressure, and heat capacity) and transport properties (such as viscosity and thermal conductivity). In previous work, some of these properties for important kerosene-based fuels have already been studied.[7–12] From such property measurements, an equation of state can be developed for a fuel. The equation of state correlates the property data and facilitates design and operational specifications for further application of the fuel. A related avenue for research is the development of surrogate fuels, which are relatively simple mixtures (often containing less than a dozen components) that approximate the behavior of a "real" kerosene fuel. Because of their relative simplicity, such surrogate fuels are useful for studying and modeling fuel behavior.[6,13,14]

Recently, physical property measurements and models for kerosene-based fuels have become necessary at temperatures greater than 300 °C and pressures greater than 10 MPa, areas in which data are scarce.[11] Under these conditions, decomposition of the fluid is a serious concern because it can affect the validity of the data that are obtained and the performance, lifetime, and safety of the instruments used to collect the data. Obviously, the extent of decomposition that occurs during thermal equilibration and property measurement has a direct impact on data quality. Additionally, decomposition of kerosene-based fuels can lead to the formation of solid deposits[15–18] that may affect instrument performance and may be difficult to remove. Changes in composition can also result in catastrophic increases in pressure. Recent work on kerosene-based fuels clearly validates such concerns for property measurements at high temperature and pressure.[19–22]

When planning property measurements, it is very useful to know the Arrhenius parameters for decomposition, which can be used to predict decomposition rates at any given temperature. The Arrhenius parameters are determined from a plot of the rate constant for decomposition as a function of the temperature.[19,23–27] In the case of complex mixtures like Jet A, rate constants for decomposition (and the Arrhenius parameters determined from them) will necessarily be approximate because they describe a complex series of reactions.[19] Nevertheless, we have found that such approximations still yield information that is useful for determining residence-time constraints on measurements conducted at high temperature and pressure.

The thermal decomposition kinetics of Jet A were determined using a method that we previously developed for the kerosene-based rocket propellant RP-1 and a series of organic Rankine cycle fluids.[19,23] With this method, the fuel is decomposed in ampule reactors made of 316 L stainless steel, and the extent of decomposition is determined as a function of time by gas chromatography. The resulting data are used to derive global pseudofirst-order rate constants that approximate the overall decomposition rate of the mixture. Rate constants for Jet A decomposition were determined at temperatures from 375 to 450 °C and were used to estimate Arrhenius parameters for the prediction of rate constants at other temperatures. While the primary purpose of this work was to establish operating ranges for the property measurements, the results clearly have implications in other facets of Jet A application. These applications include establishing operating ranges for supercritical fluid heat sink regimes, setting residence times in motors, etc.

Theory. The simplest type of decomposition is a first-order reaction in which a reactant (A) thermally decomposes into a

* To whom correspondence should be addressed. Tel.: (303) 497-5158. Fax: (303) 497-5927. E-mail: bruno@boulder.nist.gov.

10.1021/ie8000666
Published on Web 06/04/2008

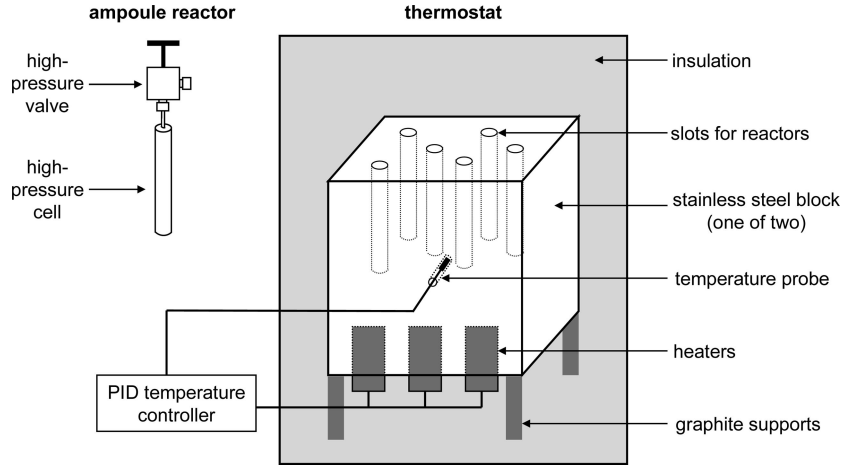

Figure 1. Apparatus used to thermally stress and decompose Jet A.

product (B); see eq 1. The rate law for such a reaction can be written in terms of the reactant or the product (eq 2), where [A] is the concentration of A, [B] is the concentration of B, k is the reaction rate constant, and t is the time. As the reaction proceeds, the decrease in [A] is accompanied by a corresponding increase in [B]. Equation 3 shows the integrated expression in terms of the products, where $[B]_t$ is the concentration of product at time t and $[B]_\infty$ is the product concentration at $t = \infty$.

$$A \rightarrow B \tag{1}$$

$$-d[A]/dt = d[B]/dt = kt \tag{2}$$

$$[B]_t = [B]_\infty(1 - \exp^{-kt}) \tag{3}$$

The thermal decomposition of a mixture like Jet A is much more complex than the reaction shown in eq 1. There are a large number of reactants, the reactants may decompose by more than one reaction pathway, the decomposition reactions may yield more than one product (disproportionation), and the initial decomposition products may further decompose to other products. Also, the decomposition rate of a single component can be significantly altered in a mixture compared to that of the pure component.[28] Consequently, a component-by-component analysis of the decomposition kinetics of Jet A would not be practical. Therefore, a simplifying assumption is necessary in order to gain insight into the overall thermal stability of Jet A. Specifically, we treat the kinetics as if dealing with a simple first-order reaction described by eq 1. This is justifiable if trends in the measured data are appropriate (see the Results and Discussion section).[29] Thus, rather than describing the decomposition of each component in the mixture, a global pseudo-first-order rate constant is derived that describes the bulk behavior of the complex fluid.[30,31]

The half-life, $t_{0.5}$, of a decomposition reaction is the time required for one-half of the reactants to become products. For a first-order reaction like the one shown in eq 1, the half-life is independent of the initial concentration and can be calculated directly from the rate constant, eq 4:

$$t_{0.5} = 0.6931/k \tag{4}$$

A related quantity is the time it takes for 1% of the reactants to become products, $t_{0.01}$. For first-order reactions, $t_{0.01}$ is also independent of the initial concentration and can be calculated directly from the rate constant, eq 5:

$$t_{0.01} = 0.01005/k \tag{5}$$

The $t_{0.5}$ and $t_{0.01}$ of thermal decomposition are useful because they give a direct measure of the time period over which the concentration of thermal decomposition products will reach an unacceptable level. Hence, they are useful when deciding what conditions and protocols are to be used for property measurements.

In addition to calculating values for $t_{0.5}$, rate constants determined at various temperatures can be used to evaluate the parameters of the Arrhenius equation, eq 6 below, where A is the pre-exponential factor, E_a is the activation energy, R is the gas constant, and T is the temperature. The Arrhenius parameters can then be used to predict rate constants at temperatures other than those examined experimentally:

$$k = A \exp(-E_a/RT) \tag{6}$$

Experimental Section

Chemicals. Reagent-grade acetone, toluene, and dodecane were obtained from commercial sources. All had purities ≥99% and were used as received. A blended sample of Jet A was obtained from the Fuels Branch of the Air Force Research Laboratory (AFRL, Wright Patterson Air Force Base). The blend was made by mixing five U.S. Jet A fuels from different manufacturers (the identification number of this mixture is POSF 4658).[32]

Apparatus. The apparatus used for the decomposition reactions is shown in Figure 1. Two thermostatted blocks of 304 stainless steel (AISI designation) were used to control the reaction temperature. Each block was supported in the center of an insulated box on carbon rods, which were chosen for their low thermal conductivity. A proportional−integral−derivative controller used feedback from a platinum resistance thermometer to maintain the temperature within 1 °C of the set value. As many as six stainless steel ampule reactors could be placed into tight-fitting holes in each of the thermostatted blocks. The ampule reactors consisted of a tubular cell with a high-pressure valve. Each cell was made from a 5.6 cm length of ultrahigh-pressure 316 L stainless steel tubing (0.64 cm external diameter and 0.18 cm internal diameter) that was sealed on one end with a 316 L stainless steel plug welded by a clean tungsten inert gas (TIG) process. The other end of each cell was connected to a valve with a 3−4 cm length of narrow-diameter 316 stainless steel tubing (0.16 cm external diameter and 0.02 cm internal diameter) that was TIG-welded to the larger diameter tube. The valves were appropriate for high temperature in that the seats were stainless steel and the packings were flexible graphite. Each cell and valve was capable of withstanding a pressure in excess

of 105 MPa at the temperatures used. The internal volume of each cell, including the short length of narrow connecting tubing, but not including the relatively small noxious volume (i.e., swept dead volume) of the valve, was determined gravimetrically from the mass of toluene required to fill it. Each cell volume was determined two or three times, and the average value (typically about 0.11 mL) was used for subsequent calculations.

Decomposition Reactions. In previous work, we demonstrated that the effect of pressure on the decomposition kinetics is small, as demonstrated by Gibbs free energy minimization calculations.[23] Nevertheless, the procedure used to fill the ampule reactors was designed to achieve an initial target pressure of 34.5 MPa (5000 psi) for all of the decomposition reactions.[19] This is important because it mimics the high-pressure conditions during some physical property measurements, and it makes the measurements more systematic. With an equation of state for *n*-dodecane, a computer program[33] calculated the mass of *n*-dodecane needed to achieve a pressure of 34.5 MPa at a given temperature and cell volume. We then assumed that the same mass of Jet A would yield a pressure close to our target pressure. This is a reasonable assumption because, although Jet A is composed of many compounds, models derived from the properties of *n*-dodecane have been used successfully to approximate the physical properties of kerosene-based fuels.[34,35] The calculated mass of Jet A was added to the cell with a syringe equipped with an ultrafine needle (sample masses were typically on the order of 0.06 g and varied depending on the experimental temperature and cell volume). The valve was then affixed to the cell and closed. Cells were then chilled to 77 K in liquid nitrogen and subsequently evacuated to 10 Pa through the valve to remove air from the cell. The valve was then reclosed, and the cell was warmed to room temperature. The single freeze−pump−thaw cycle should remove the air from the vapor space in the cell without removing dissolved air from the fuel itself. This mimics the conditions under which a "real" jet fuel is used (i.e., it will contain dissolved air). The other advantage of doing only one freeze−pump−thaw cycle is that it limits the chances of removing more volatile components from the fuel. More rigorous degassing procedures, such as bubbling inert gas through the fuel, will cause a change in fuel composition by removing some of the more volatile components from the fuel. It is also worth mentioning that the auto-oxidation reactions caused by dissolved oxygen are thought to be relatively unimportant for hydrocarbon fuel decomposition above 250−300 °C.[18]

Loaded ampule reactors were then inserted into the thermostatted stainless steel block, which was maintained at the desired reaction temperature. Fluid reflux inside the cells was minimized by putting the entire ampule reactor inside the insulated box (although only the cell tubing was inserted into the thermostatted block). The ampule reactors were maintained at the reaction temperature for a specified period of time ranging from 10 min to 24 h. In order to minimize the time required for temperature equilibration, only one reactor at a time was placed in the thermostatted block if the reaction time was shorter than 30 min. After decomposition, the reactors were removed from the thermostatted block and immediately cooled in room-temperature water. The thermally stressed Jet A was then recovered and analyzed as described below.

After each run, the cells and valves were rinsed extensively with a mixture of acetone and toluene. The cells were also sonicated for about 5 min (while filled with the acetone/toluene mixture) between rinsings in order to remove any solid deposits that may have formed on their walls. Cleaned cells and valves were heated to 150 °C for at least 1 h to remove residual solvent.

Blank experiments were occasionally performed to check the effectiveness of this protocol for cleaning the cells. For these blank experiments, a cell was loaded with Jet A as described above, but the cell was not heated above room temperature. After about a day, the Jet A in the cell was removed and analyzed by gas chromatography (as described in the following section). The success of the cleaning procedure was confirmed by the visual absence of color or solids in the unheated Jet A and by the absence of decomposition products in the resulting gas chromatogram.

Analysis of Liquid-Phase Decomposition Products. The production of light decomposition products caused the pressure in the ampule reactors to increase during the decomposition reactions. After decomposition, the ampule reactors contained a pressurized mixture of vapor and liquid, even at room temperature. Liquid-phase decomposition products in the thermally stressed Jet A were used to monitor the kinetics of decomposition. Therefore, a sampling procedure was designed to minimize loss of the liquid sample when the ampule reactors were opened. Specifically, a short length of stainless steel tubing was connected to the valve outlet on the ampule reactor. The end of this tubing was placed inside a chilled (7 °C) glass vial, and the valve was slowly opened. All, some, or none of the reacted Jet A was expelled into the vial, depending on the pressure in the reactor. The valve was then removed from the reactor and any liquid remaining in the cell was transferred to the glass vial using a syringe with an ultrafine needle. The vial was sealed with a silicone septum closure, and the mass of liquid sample was quickly determined (with an uncertainty of 0.0001 g). The liquid sample was immediately diluted with a known amount of *n*-dodecane and refrigerated (at 7 °C) until the analysis was performed. The purpose of this procedure was to prepare the samples for GC analysis and to minimize evaporative losses from the samples. The resulting *n*-dodecane solution was typically 5% reacted Jet A (mass/mass).

Aliquots (3 μL) from crimp-sealed vials of each sample were injected into a gas chromatograph equipped with an automatic sampler and a flame ionization detector. Research-grade nitrogen was used as the carrier and makeup gas. The split/splitless injection inlet was maintained at 300 °C, and samples were separated on a 30 m capillary column coated with a 0.1 μm film of (5%-phenyl)methylpolysiloxane. A temperature program was used that consisted of an initial isothermal separation at 80 °C for 4 min, followed by a 20 °C/min gradient to 275 °C. This final temperature was held constant for 4 min.

Jet A decomposition was observed from the increase in the chromatographic signal of certain decomposition products. For the kinetic analysis, a detailed identification of each product is unnecessary; only the rate of composition change is required. Chromatograms of unreacted Jet A exhibited no (or very small) peaks below a retention time of 2.8 min, whereas after reaction, a suite of decomposition products was observed to elute earlier than 2.8 min. The total peak area of this emergent suite of decomposition products was used for the kinetic analysis of decomposition. The peak area was corrected for dilution in *n*-dodecane by multiplying by the dilution factor. The peak area was also corrected for drifts in detector response by analyzing an aliquot of a stock solution (pentane and hexane in *n*-dodecane) along with each set of decomposition samples. Using the corrected peak areas as $[B]_t$, the kinetic data for each temperature were fit to eq 3 with a nonlinear least-squares program. Because of secondary decomposition (and long

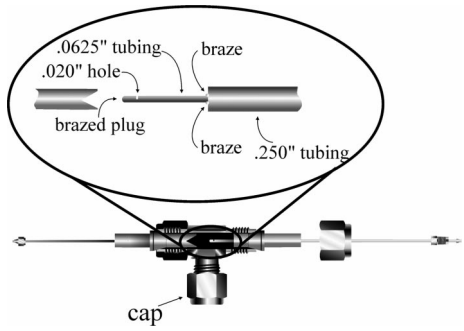

Figure 2. Gas−liquid separation device.

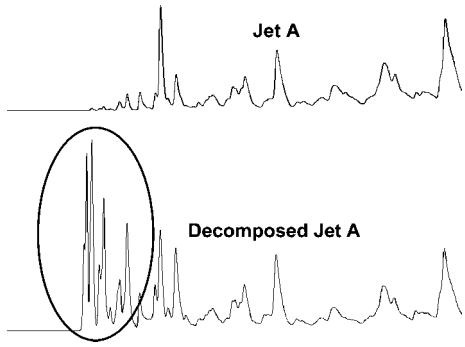

Figure 3. Initial part of the gas chromatograms for Jet A and for a sample of decomposed Jet A that had been thermally stressed at 450 °C for 40 min. The emergent suite of liquid decomposition products that was used for the kinetic analysis is circled.

reaction times at the lower temperatures), it was not possible to determine experimentally a value for $[B]_\infty$. The recommended[36] procedure in such an instance is to treat $[B]_\infty$ as a floating variable (along with k) when fitting the kinetic data, which is what was done.

In order to limit the influence of any secondary decomposition reactions on the kinetics, we used only the initial, rapidly changing part of the kinetic curve to determine k. Specifically, at 375 °C, the data points used to determine k corresponded to decomposition reactions ranging from 4 to 24 h. At 400 °C, the data points used to determine k corresponded to decomposition reactions ranging from 1 to 4 h. At 425 °C, the data points used to determine k corresponded to decomposition reactions ranging from 0.5 to 2 h. At 450 °C, the data points used to determine k corresponded to decomposition reactions ranging from 10 to 40 min.

Analysis of Vapor-Phase Decomposition Products. While the rate constants reported here were determined exclusively from decomposition products found in the liquid phase, a noticeable vapor phase was generated in most of the experiments. This vapor phase could have a significant pressure, although we estimate that the vapor mole fraction was small compared to that of the total product suite.[19] Nevertheless, we wanted to obtain some understanding of the vapor-phase composition.

To obtain a chemical analysis of the vapor phase, we used a gas−liquid separator that was designed and built previously; see Figure 2.[37] This device, which is similar in concept to branch-point separators in natural gas transmission lines, was constructed from a 316 stainless steel T fitting. The effectiveness of branch-point separators is due to the volume change in the enclosure of the separator and to the position of the vapor-collection tube. Similarly, the device shown in Figure 2 effectively strips off the liquid phase from the vapor. This

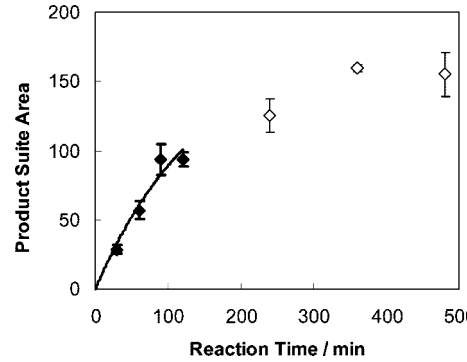

Figure 4. Plot of the corrected area counts of the decomposition product suite as a function of time at 425 °C. Only the data at short reaction times (solid symbols) were used to determine the rate constant. The error bars represent the standard deviation for replicate decomposition reactions at each time point.

allowed us to independently analyze the vapor phase using a gas chromatograph with MS detection. The vapor from a separate decomposition experiment at 450 °C was introduced directly into the split/splitless injection port of the chromatograph by flowing capillary injection,[38] and was separated on a 30 m capillary column coated with a 0.25 μm film of (5%-phenyl)methylpolysiloxane. A temperature program was used to separate the sample with an initial isothermal separation at 35 °C for 5 min, followed by a 10 °C/min ramp to 200 °C. MS spectra were recorded for fragments of relative molecular mass from 18 to 550.

Results and Discussion

Considerable batch-to-batch variation in the composition of Jet A can be expected.[10,32] This variation has the potential to affect the thermal decomposition kinetics of Jet A. To illustrate, the rate constants for the thermal decomposition kinetics of different batches of kerosene-based rocket propellant differed by as much as a factor of 6.[19] To compensate for this potential variability, we used an "average" Jet A that had been made by blending together five U.S. Jet A fuels from different manufacturers.[32] The composition of this mixture has been shown to be representative of an average jet fuel.[32] The most abundant constituents in this mixture of Jet A, which account for about 40% of the sample, are shown in Table 1.[10] The expectation is that, by using this blended sample of Jet A fuels, the resulting rate constants for thermal decomposition will be near the average value for the individual samples.

Aliquots of the blended Jet A were decomposed in stainless steel ampule reactors at 375, 400, 425, and 450 °C. This temperature range was chosen because it allowed for reaction times of a convenient length. At 375 °C, the reaction is relatively slow, so reaction times ranged from 4 to 24 h. At 450 °C, the reaction is much faster, so reaction times ranged from 10 to 120 min.

The unreacted Jet A was clear and nearly colorless. Mild thermal stress (i.e., the shortest reaction times at the lower temperatures) caused the liquid to become pale yellow. Severe thermal stress (i.e., the longest reaction times at the higher temperatures) caused the liquid to become very dark brown, opaque, and viscous. A small amount of dark particulate was regularly seen in the more thermally stressed samples. Additionally, low-molecular-weight decomposition products caused a pressurized vapor phase to develop inside the reactors. For the more severely stressed samples, it was common for the entire liquid sample to be expelled under pressure when the reactor valve was opened.

Table 1. By GC-MS, These Are the Most Abundant Constituents in the Sample Of Jet A Used in This Work; The "Area Percentage" Refers to the Relative Area of Each Peak in a Plot of the Total Ion Current from the MS Detector As a Function Of Time (When Ambiguity Exists Regarding Isomerization, The Substituent Position Is Indicated with an *x*)

name	CAS no.	area percentage	name	CAS no.	area percentage
n-heptane	142-82-5	0.125	2,3-dimethyl decane	17312-44-6	0.681
ethyl cyclohexane	108-87-2	0.198	1-ethyl-2,2,6-trimethyl cyclohexane	71186-27-1	0.364
2-methyl heptane	592-27-8	0.202	1-methyl-3-propyl benzene	1074-43-7	0.569
toluene	108-88-3	0.320	aromatic	NA	0.625
cis-1,3-dimethyl cyclohexane	638-04-0	0.161	5-methyl decane	13151-35-4	0.795
n-octane	111-65-9	0.386	2-methyl decane	6975-98-0	0.686
1,2,4-trimethyl cyclohexane	2234-75-5	0.189	3-methyl decane	13151-34-3	0.969
4-methyl octane	2216-34-4	0.318	aromatic	NA	0.540
1,2-dimethyl benzene	95-47-6	0.575	aromatic	NA	0.599
n-nonane	111-84-2	1.030	1-methyl-(4-methylethyl) benzene	99-87-6	0.650
x-methyl nonane	NA	0.597	*n*-undecane	1120-21-4	2.560
4-methyl nonane	17301-94-9	0.754	*x*-methyl undecane	NA	1.086
1-ethyl-3-methyl benzene	620-14-4	1.296	1-ethyl-2,3-dimethyl benzene	933-98-2	1.694
2,6-dimethyl octane	2051-30-1	0.749	*n*-dodecane	112-40-3	3.336
1-methyl-3-(2-methylpropyl) cyclopentane	29053-04-1	0.285	2,6-dimethyl undecane	17301-23-4	1.257
1-ethyl-4-methyl benzene	622-96-8	0.359	*n*-tridecane	629-50-5	3.998
1-methyl-2-propyl cyclohexane	4291-79-6	0.370	1,2,3,4-tetrahydro-2,7-dimethyl naphthalene	13065-07-1	0.850
1,2,4-trimethyl benzene	95-63-6	1.115	2,3-dimethyl dodecane	6117-98-2	0.657
n-decane	124-18-5	1.67	2,6,10-trimethyl dodecane	3891-98-3	0.821
1-methyl-2-propyl benzene	1074-17-5	0.367	*x*-methyl tridecane	NA	0.919
4-methyl decane	2847−72−5	0.657	*x*-methyl tridecane	NA	0.756
1,3,5-trimethyl benzene	108-67-8	0.949	*n*-tetradecane	629-59-4	1.905
x-methyl decane	NA	0.613	*n*-pentadecane	629-62-9	1.345

Table 2. Summary of the Most Abundant Decomposition Products Found in the Vapor Phase after 2 h at 450 °C

compound	% of total ion current
butane	13.0
pentane	10.6
propane	10.4
2-methylpropane	8.6
2-methylbutane	8.1
ethane	6.6
hexane	6.4
2-methylpentane	5.9
methylcyclopentane	3.3
3-methylpentane	3.2

For a severely stressed sample of Jet A (2 h at 450 °C), the gas phase was separated from the liquid phase using the device shown in Figure 2. The gas phase was then analyzed using a gas chromatograph with MS detection. Over 30 compounds were identified in the gas phase, with light alkanes being the most abundant. Table 2 shows the 10 most abundant compounds, based on total ion current in the MS detector. Note that the MS method employed precludes observation of methane. The apparent lack of alkene decomposition products is somewhat surprising, although it is known that high pressures and long reaction times decrease the yield of alkenes from the decomposition of alkanes.[15,22,39]

The thermally stressed liquid phase of each sample was analyzed by a gas chromatograph equipped with a flame ionization detector. An easily identifiable suite of decomposition products had retention times between 2.3 and 2.8 min; see Figure 3. The kinetic analysis was done using this suite of peaks. We did not identify all of the individual compounds responsible for these peaks, but it is worth noting that pentane and hexane had retention times of 2.4 and 2.5 min under these conditions, which suggests that most of these decomposition products had 5−7 carbon atoms. The observed product suite was essentially the same at all temperatures, with retention times that were constant to within 0.01 min. Undoubtedly, there were peaks for decomposition products in the broad kerosene "hump" that began around 2.9 min, but using them for the kinetic analysis was impractical because of peak overlap and the lack of baseline resolution. Additionally, we did not routinely monitor compounds that were not retained in the liquid phase, including vapor-phase products and potential coke deposits.

Table 3. Kinetic Data for the Thermal Decomposition of Jet A

T/°C	k/s^{-1}	uncertainty in k/s^{-1}	$t_{0.5}$/h	$t_{0.01}$/min
375	5.9×10^{-6}	3.9×10^{-6}	33	28
400	3.3×10^{-5}	1.8×10^{-5}	5.8	5.0
425	1.2×10^{-4}	0.6×10^{-4}	1.7	1.4
450	4.4×10^{-4}	2.3×10^{-4}	0.44	0.38

As mentioned above, the kinetic analysis was done using the emergent suite of decomposition products in the liquid phase with retention times between 2.3 and 2.8 min. The rate constant, k, at each temperature was determined from data collected at four different reaction times, with 3−6 replicate decomposition reactions run at each reaction time. The value of k was obtained from a nonlinear least-squares fit of these data to eq 3. For example, Figure 4 is a plot of the data and curve-fit for 425 °C. Note that data points were collected at seven time points, but only the first four data points in Figure 4 were used to determine k. The reason for excluding the later time points was to limit the influence of any secondary decomposition reactions on the kinetics. Even though it is unlikely that measurements would intentionally be carried out with instrumental residence times in excess of the first four time points, this area of the plot is still useful in that it represents the chemical decomposition regime that is possible if an instrument or engine enters an upset condition resulting in long residence times. See the Experimental Section for a list of the reaction times used to determine the decomposition kinetics at each temperature. As described in the Theory section, values for $t_{0.5}$ and $t_{0.01}$ are calculated from k using eqs 4 and 5. The decomposition rate constants at all four temperatures, along with values of $t_{0.5}$ and $t_{0.01}$, are presented in Table 3. The standard uncertainties given in Table 3 were calculated from the standard deviation of replicate measurements and from the standard error in the nonlinear fit. The values of $t_{0.01}$ show that physical property measurements at ≥400 °C would require apparatus residence times on the order of 5 min or less. On the other hand, at 375 °C, a residence time of about one-half hour may be acceptable. First-order rate constants reported for the decomposition of *n*-tetradecane are $k = 1.78 \times 10^{-5}$ s^{-1} at 400 °C, $k = 1.01 \times 10^{-4}$ s^{-1} at 425 °C, and

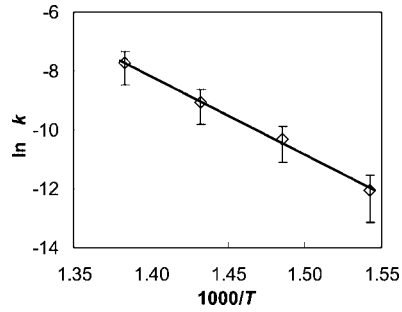

Figure 5. Arrhenius plot for the decomposition of Jet A. The Arrhenius parameters determined from the fit to the data are $A = 4.1 \times 10^{12}$ s^{-1} and $E_a = 220$ kJ·mol^{-1}.

$k = 4.64 \times 10^{-4}$ s^{-1} at 450 °C.[40] Within our experimental uncertainty, these are the same as the values in Table 3 for Jet A.

An Arrhenius plot of the rate constants is shown in Figure 5. The Arrhenius parameters determined from a linear regression of the data are $A = 4.1 \times 10^{12}$ s^{-1} and $E_a = 220$ kJ·mol^{-1}. The standard uncertainty in E_a, calculated from the standard error in the slope of the regression, is 10 kJ·mol^{-1}. The linearity of the Arrhenius plot ($r^2 > 0.99$) over the 75 °C temperature range is an important validation that the assumption of first-order kinetics is reasonable. Note that the activation energy for the decomposition of Jet A is slightly lower than the values reported for pure C_{10}−C_{14} *n*-alkanes; for example, for *n*-dodecane E_a is 260 kJ·mol^{-1} (with a reported uncertainty of 8 kJ·mol^{-1}).[40]

The rate of decomposition and the product suite from alkane decomposition are known to have some dependence on the material used to construct the reactor.[22] This suggests that surface catalysis of decomposition can be important for at least some reactor materials. As discussed in the Introduction, one of our goals in doing this decomposition study is so that we can avoid significant decomposition during high-temperature property measurements in various instruments. However, if surface catalysis is important, the decomposition rate will be different in every instrument. So, how can we use the decomposition rates measured in the ampule reactors? First, we purposefully used reactors with a high ratio of surface area to volume, so that any effect of surface catalysis will be magnified. This way, if the rate of decomposition is actually different in another instrument, it will be slower, which does not create a problem. Second, we directly checked the importance of surface catalysis by performing two decomposition reactions in a stainless steel ampule reactor with a larger internal diameter. This reactor has a surface area-to-volume ratio that is 40% lower than in our standard reactors. However, the rate of decomposition did not change observably in the lower-surface-area reactor, which suggests that surface catalysis is not very important in this system.

A related issue is the possibility that the surface properties of the reactors could change with age and use. This could potentially change the amount of surface-catalyzed decomposition and cause a shift in the observed rate constants for decomposition. Our experimental design accounts for such a possibility in the following way. At any one time, we have a set of about 15 reactors that are used for decomposition studies. Individual reactors occasionally fail (by developing a leak, etc.) and are replaced by new reactors. Consequently, the reactors that we used for this decomposition study were of varying ages. Additionally, the different temperatures and reaction times were not done in a particular order. Consequently, any effects of reactor aging should already be observable as scatter in the data (and, therefore, included in the uncertainty estimates for the rate constants). Since scatter in the data is not that great, we conclude that surface aging in the reactors is not that important in this system.

Conclusions

By assuming first-order kinetics, we find that Jet A has a thermal stability that is similar to that of C_{10}−C_{14} *n*-alkanes. This knowledge is useful for planning physical and chemical property measurements at high temperatures and pressures. On the basis of the amount of time required for 1% of the sample to decompose ($t_{0.01}$), we found that allowable instrument residence times ranged from about 0.5 h at 375 °C to <1 min at 450 °C. An important caveat for this conclusion is that the kinetics of decomposition may depend on the identity of the wetted surfaces of the apparatus or container. Strictly speaking, these results are best applied when the wetted surface is constructed from 300 series stainless steels.

Acknowledgment

We acknowledge the financial support of the Air Force Office of Scientific Research (MIPR F1ATA06004G004).

Literature Cited

(1) Aviation Turbine Fuels. Air BP Handbook of Products. http://www.bp.com/sectiongenericarticle.do?categoryId=4503702&contentId=57750 (accessed in 2007).

(2) *Handbook of Aviation Fuel Properties*, 3rd ed.; Coordinating Research Council, Inc.: Alpharetta, GA, 2004.

(3) Edwards, T. Advancements in gas turbine fuels from 1943 to 2005. *J. Eng. Gas Turbines Power* **2007**, *129*, 13–20.

(4) Maurice, L. Q.; Lander, H.; Edwards, T.; Harrison, W. E. Advanced aviation fuels: A look ahead via a historical perspective. *Fuel* **2001**, *80*, 747–756.

(5) Edwards, T. "Kerosene" Fuels for Aerospace Propulsion—Composition and Properties. Presented at 38th AIAA/ASME/SAE/ASEE Joint Propulsion Conference & Exhibit, Indianapolis, IN, 2002; Paper 3874.

(6) Wang, T. S. Thermophysics characterization of kerosene combustion. *J. Thermophys. Heat Transfer* **2001**, *15*, 140–147.

(7) Bruno, T. J.; Huber, M. L.; Laesecke, A.; Lemmon, E. W.; Perkins, R. A. *Thermochemical and Thermophysical Properties of JP-10*; NISTIR 6640; National Institute of Standards and Technology: Boulder, CO, 2006.

(8) Bruno, T. J.; Smith, B. L. Improvements in the measurement of distillation curves. 2. Application to aerospace/aviation fuels RP-1 and S-8. *Ind. Eng. Chem. Res.* **2006**, *45*, 4381–4388.

(9) Magee, J. W.; Bruno, T. J.; Friend, D. G.; Huber, M. L.; Laesecke, A.; Lemmon, E. W.; McLinden, M. O.; Perkins, R. A.; Baranski, J.; Widegren, J. A. *Thermophysical Properties Measurements and Models for Rocket Propellant RP-1: Phase I*; NISTIR 6646; National Institute of Standards and Technology: Boulder, CO, 2007.

(10) Smith, B. L.; Bruno, T. J. Improvements in the measurement of distillation curves. 4. Application to the aviation turbine fuel Jet-A. *Ind. Eng. Chem. Res.* **2007**, *46*, 310–320.

(11) *Liquid Propellant Manual*; Chemical Propulsion Information Agency: Columbia, MD, 1997.

(12) Bruno, T. J. *The Properties of S-8 and JP-10*; Technical Report to the Wright Laboratory Aero Propulsion and Power Directorate; National Institute of Standards and Technology: Boulder, CO, Nov 2007.

(13) Edwards, T. "Real" kerosene aviation and rocket fuels: Composition and surrogates. *Chem. Phys. Process. Combust.* **2001**, *17*, 276–279.

(14) Edwards, T.; Maurice, L. Q. Surrogate mixtures to represent complex aviation and rocket fuels. *J. Propul. Power* **2001**, *17*, 461–466.

(15) Edwards, T. Cracking and deposition behavior of supercritical hydrocarbon aviation fuels. *Combust. Sci. Technol.* **2006**, *178*, 307–334.

(16) Edwards, T.; Zabarnick, S. Supercritical Fuel Deposition Mechanisms. *Ind. Eng. Chem. Res.* **1993**, *32*, 3117–3122.

(17) Bates, R. W.; Edwards, T. Heat Transfer and Deposition Behavior of Hydrocarbon Rocket Fuels. Presented at 41st Aerospace Sciences Meeting and Exhibit, Reno, NV, 2003; Paper 123.

(18) Watkinson, A. P.; Wilson, D. I. Chemical reaction fouling: A review. *Exp. Therm. Fluid Sci.* **1997**, *14*, 361–374.

(19) Andersen, P. C.; Bruno, T. J. Thermal decomposition kinetics of RP-1 rocket propellant. *Ind. Eng. Chem. Res.* **2005**, *44*, 1670–1676.

(20) Stiegemeier, B.; Meyer, M. L.; Taghavi, R. A. Thermal Stability and Heat Transfer Investigation of Five Hydrocarbon Fuels: JP-7, JP-8, JP-8 + 100, JP-10, RP-1. Presented at 38th AIAA/ASME/SAE/ASEE Joint Propulsion Conference & Exhibit, Indianapolis, IN, 2002; Paper 3873.

(21) Wohlwend, K.; Maurice, L. Q.; Edwards, T.; Striebich, R. C.; Vangsness, M.; Hill, A. S. Thermal stability of energetic hydrocarbon fuels for use in combined cycle engines. *J. Propul. Power* **2001**, *17*, 1258–1262.

(22) Yu, J.; Eser, S. Thermal decomposition of $C_{10}-C_{14}$ normal alkanes in near-critical and supercritical regions: Product distributions and reaction mechanisms. *Ind. Eng. Chem. Res.* **1997**, *36*, 574–584.

(23) Andersen, W. C.; Bruno, T. J. Rapid screening of fluids for chemical stability in organic rankine cycle applications. *Ind. Eng. Chem. Res.* **2005**, *44*, 5560–5566.

(24) Bruno, T. J.; Hume, G. L. A High-Temperature, High-Pressure Reaction-Screening Apparatus. *J. Res. Natl. Bur. Stand. (U.S.)* **1985**, *90*, 255–257.

(25) Bruno, T. J.; Straty, G. C. Thermophysical property measurement on chemically reacting systems—A case study. *J. Res. Natl. Bur. Stand. (U.S.)* **1986**, *91*, 135–138.

(26) Straty, G. C.; Ball, M. J.; Bruno, T. J. PVT of Toluene at Temperatures to 673 K. *J. Chem. Eng. Data* **1988**, *33*, 115–117.

(27) Straty, G. C.; Palavra, A. M. F.; Bruno, T. J. PVT Properties of Methanol at Temperatures to 300 °C. *Int. J. Thermophys.* **1986**, *7*, 1077–1089.

(28) Yu, J.; Eser, S. Supercritical-phase thermal decomposition of binary mixtures of jet fuel model compounds. *Fuel* **2000**, *79*, 759–768.

(29) House, J. E. *Principles of Chemical Kinetics*; William C. Brown Publishers, Times Mirror Higher Education Group, Inc.: Dubuque, IA, 1997.

(30) Fodor, G. E.; Naegeli, D. W.; Kohl, K. B. Peroxide Formation in Jet Fuels. *Energy Fuels* **1988**, *2*, 729–734.

(31) Lorant, F.; Behar, F.; Vandenbroucke, M.; McKinney, D. E.; Tang, Y. C. Methane generation from methylated aromatics: Kinetic study and carbon isotope modeling. *Energy Fuels* **2000**, *14*, 1143–1155.

(32) Shafer, L. M.; Striebich, R. C.; Gomach, J.; Edwards, T. Chemical Class Composition of Commercial Jet Fuels and Other Specialty Kerosene Fuels. Presented at 14th AIAA/AHI Space Planes and Hypersonic Systems and Technologies Conference, Canberra, Australia, 2006; Paper 2006-7972.

(33) Lemmon, E. W.; McLinden, M. O.; Huber, M. L. *REFPROP, Reference Fluid Thermodynamic and Transport Properties, version 7*; NIST Standard Reference Database 23; National Institute of Standards and Technology: Gaithersburg, MD, 2002.

(34) Huber, M. L.; Laesecke, A.; Perkins, R. Transport properties of *n*-dodecane. *Energy Fuels* **2004**, *18*, 968–975.

(35) Lemmon, E. W.; Huber, M. L. Thermodynamic properties of *n*-dodecane. *Energy Fuels* **2004**, *18*, 960–967.

(36) Espenson, J. H. *Chemical Kinetics and Reaction Mechanisms*, 2nd ed.; McGraw-Hill: New York, 1995; p 25.

(37) Bruno, T. J. Conditioning of flowing multiphase samples for chemical analysis. *Sep. Sci. Technol.* **2005**, *40*, 1721–1732.

(38) Bruno, T. J. *Handbook for the Analysis and Identification of Alternative Refrigerants*; CRC Press: Boca Raton, FL, 1995.

(39) Wojciechowski, B. W.; Corma, A. *Catalytic Cracking: Catalysts, Chemistry, and Kinetics*; Marcel Dekker, Inc.: New York, 1986.

(40) Yu, J.; Eser, S. Kinetics of supercritical-phase thermal decomposition of $C_{10}-C_{14}$ normal alkanes and their mixtures. *Ind. Eng. Chem. Res.* **1997**, *36*, 585–591.

Received for review January 15, 2008
Revised manuscript received April 1, 2008
Accepted April 3, 2008

IE8000666